Effect of Synthesis Temperature on Adsorbent Performance of Blending Anionic and Cationic Gels in Divalent Metal Ions Adsorption

Eva Oktavia Ningrum*, Suprapto Suprapto, Saidah Altway, Warlinda Eka Triastuti, Afan Hamzah, Agus Surono, Lulu Sekar Taji, and Erlangga Ardiansyah

Department of Industrial Chemical Engineering, Faculty of Vocational Studies, Institut Teknologi Sepuluh Nopember, Kampus ITS Sukolilo, Surabaya 60111, Indonesia

Abstract: *In this study, the anionic and cationic gels were synthesized separately using copolymerization between* N-*isopropylacrylamide (NIPAM) and acrylic acid or chitosan through a polymerization reaction using* N,N'-*methylenebisacrylamide (MBAA) as a cross-linker with various monomer concentrations and synthesis temperature. The anionic and cationic gels were blended to minimize inter-intra particle association and to improve the adsorption ability. The FTIR analysis found that the synthesis of the NIPAM-*co-*acrylic acid and NIPAM-*co-*chitosan gels was successfully carried out, indicating no presence of a vinyl group in the functional group. The result showed that the ion adsorption amount of Pb²⁺ ions blending gels increased significantly, almost twice compared to the adsorption before blending. The adsorption amount of Pb²⁺ ions increased with increasing the gel synthesis temperature. The adsorption amount follows the order of $Pb^{2+} > Fe^{2+} > Ni^{2+}$. The adsorption amount of Pb²⁺ tends to decrease with increasing sedimentation volume. The higher the synthesis temperature, the larger the porous diameter formed. These results demonstrate that blending gel of NIPAM-*co-*chitosan and NIPAM-*co-*acrylic acid is a feasible alternative for removing heavy metal ions owing to its good adsorption performance.*

Keywords: *anionic and cationic gel; adsorption amount; NIPAM-*co-*acrylic acid; NIPAM-*co-*chitosan*

■ INTRODUCTION

The need for electroplating goods has expanded due to the quick development of technology in fields including the automobile sector, electrical devices, construction, and others. At the same time, waste comprising heavy metal ions is created during the electroplating process. Heavy metal ions become a major hazard if waste is disposed of without any treatment. Since heavy metal ions cannot be naturally degraded, they constitute a type of B3 waste that can harm aquatic ecosystems and the surrounding human population [1].

The Buyat Bay pollution case was one instance of heavy metal ion contamination that garnered attention in Indonesia between 1996 and 2004. The marine environment in Buyat Bay was badly harmed by the pollution caused by PT. Newmont Minahasa Raya's extensive mining operations resulted in the daily dumping of 2,000 tons of tailings [2]. In research by Tamburini et al. [3] in North Sulawesi Province, samples were taken downstream from four mining zones to four control locations. At mine discharge locations compared to control sites, mean concentrations of arsenic (As), gold (Au), cobalt (Co), chromium (Cr), copper (Cu), mercury (Hg), nickel (Ni), lead (Pb), antimony (Sb), and zinc (Zn) in sediments were considerably higher. Holothurians were discovered to have significantly greater amounts of As, Au, Cr, Hg, and Ni in their body walls and As, Au, Co, Cr, Cu, Hg, Pb, Sb, Sn, and Zn in their guts when compared to control locations downstream of gold mines. The location next to the oldest artisanal mine had higher contamination levels in the sediments and tissues.

Heavy metal ions have been recovered from solutions using various traditional techniques; however, these techniques have flaws. Precipitation and flotation are two techniques that create a lot of secondary waste and are unprofitable due to their high operational costs. Additionally, the coagulation process generates sludge, and the regeneration of the resin in ion exchange needs strong acids [4]. The most efficient and cost-effective approach of the ones mentioned above is adsorption, particularly biosorption [5]; nevertheless, they are not reusable and provide additional disposal issues [6]. The adsorbent's inherent properties displayed the essential element for the efficient adsorption of the metal ions. Due to the insufficient adsorption capacity and slow adsorption rate of common absorbents, various obstacles still limit the adsorption approach. The importance of new adsorbent materials for heavy-metal ion removal with high adsorption capacities and quick adsorption rates must be considered. When examining the sensitivity, selectivity, adsorption, and reusability, the use of certain functional organic ligands highlights the metal ions under specific circumstances and reduces the amount of experimental work required. It has been found that several organic materials, nanomaterials, and metal-organic frameworks have good kinetic performances and exhibit high Pb(II) ion adsorption rates [7-17]. However, it has continued to be difficult to regenerate conjugate adsorbent using strong acid, which produces secondary waste.

One of the most recent adsorption techniques for removing heavy metals is a thermosensitive gel based on zwitterionic betaine [18-21]. Zwitterionic betaine effectively regenerates heavy metal ions because of the interaction between ions and their positive and negative groups. Additionally, in our earlier research [20,22-24], gels made from the copolymerization of zwitterionic betaine and NIPAM demonstrate the capability of reversible heavy metal ion adsorption and desorption by temperature change. One disadvantage of the zwitterionic betaine gel adsorption approach is the presence of inter-intrachain connections, which restrict the gel's capacity to adsorb heavy metal ions. Therefore, an alternative adsorbent that is environmentally friendly is needed, i.e.,

does not cause secondary waste as adsorbent regeneration only by temperature change and has a high adsorption capacity. The alternative proposed in this study is copolymer gel based on NIPAM-*co*-chitosan and NIPAM-*co*-acrylic acid. Acrylic acid and chitosan have adsorption abilities because they have ionic groups, while NIPAM can desorb ions because it is thermosensitive. At high temperatures, NIPAM is hydrophobic however it is hydrophilic at low temperatures. So, the copolymerization of the two compounds is advantageous regarding their adsorption and desorption capabilities (reversible) and occurs simultaneously. In addition, this adsorbent is economical and environmentally friendly due to the biodegradable properties of chitosan and acrylic acid. This study is expected to provide information regarding developing zero-waste technology and alternative adsorbents with superior properties. Based on the above background, the problem to be discussed in this study is the copolymerization of sulfobetaine zwitterionic polymers and thermosensitive gels, which several previous researchers have carried out. It is well known that the interaction of the charge group limits adsorption in the zwitterionic gel. To avoid this association, the gel will be synthesized separately using NIPAM-*co*-chitosan, which tends to contain positively charged ions, and NIPAM-*co*-acrylic acid, which carries negatively charged ions. So, when the gel is used for the adsorption of heavy metal waste, it will result in competition between each ion from the polymer and the ions in the waste solution.

In addition, chitosan is a material that is easily found in nature. Chitosan is biodegradable; thus, it can be decomposed in nature and does not cause pollution detrimental to the environment, humans, and surrounding living things. So, research on NIPAM-*co*-chitosan and NIPAM-*co*-acrylic acid gels needs to be carried out to reduce heavy metal waste and not produce secondary waste, which can damage the environment in the presence of biodegradable properties of chitosan. This study aims to evaluate the adsorption amount of heavy metal ions by NIPAM-*co*-chitosan and NIPAM-*co*-acrylic acid gels. The sedimentation volumes of

NIPAM-*co*-chitosan and NIPAM-*co*-acrylic acid gels were also investigated and correlated with the adsorption amount, along with elucidating the temperature at which the gels of NIPAM-*co*-chitosan and NIPAM-*co*-acrylic acid were synthesized affected their ability to adsorb heavy metals.

■ EXPERIMENTAL SECTION

Materials

The materials used to synthesize the gel adsorbent were NIPAM monomer obtained from KJ Chemicals Co., Japan; chitosan obtained from Acros Organics BVBA, Belgium; and acrylic acid obtained from Sigma Aldrich Co., USA. Furthermore, N,N,N',N'-tetramethylethylenediamine (TEMED) was used as an accelerator obtained from AppliChem GmbH., Germany; and sodium sulfite (Na_2SO_3) was obtained from Sigma Aldrich Co., USA. For the initiator, ammonium peroxodisulfate (APDS) was obtained from Nacalai Tesque, Inc., Japan, and ammonium persulfate (APS) was obtained from Xilong Chemical Co., China. The N,N'-methylenebisacrylamide (MBAA) cross-linker was obtained from Sigma Aldrich Co., USA. The distilled water and nitrogen gas were obtained from PT Aneka Gas Industri Tbk, Indonesia. Benzene and *n*-hexane were obtained from Sigma Aldrich Co., USA, and they were used when purifying NIPAM. The apparatus used to synthesize the anionic and cationic gel is shown in Fig. 1.

Instrumentation

FTIR analysis

Fourier-transform infrared spectroscopy (FTIR) was applied to analyze the functional groups of gel constituent monomers. METTLER TOLEDO Instrument Co., Ltd., Switzerland was employed by ATR method in wavenumbers ranges of 4000–500 cm^{-1}.

Atomic absorption spectrophotometry (AAS) analysis

The target solution's ion concentrations were measured using AAS on a Model 210 VGP from Buck Scientific in the United States. The dry gel (1 g) was placed in a glass bottle with 20 mL of a 10 mmol/L PbCl$_2$ solution to conduct the adsorption experiment. The gel-containing solution was agitated for 12 h after the bottle

1. Polymerization reactor
2. Stirrer
3. Initiator inlets
4. Nitrogen gas
5. Magnetic stirrer
6. Temperature controllers
7. Gas outlets
8. Inlet gas gauge
9. Inlet gas
10. Stative
11. Waterbath
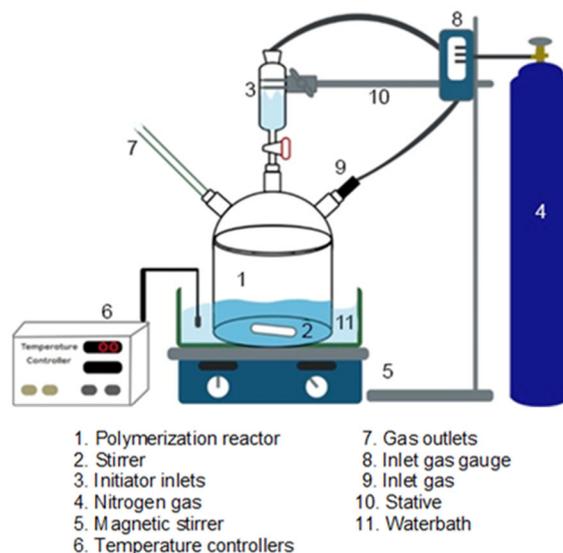
Fig 1. Schematic gel synthesis apparatus

was placed in a water bath that had been heated to the desired temperature to allow the gel to reach adsorption equilibrium. After adsorption, the gels were withdrawn from the solution and centrifuged at 3,000 rpm for 10 min to quantify the concentration of Pb^{2+} in the solution.

Sedimentation volume analysis

The sedimentation volume experiment was carried out by inserting the crushed gel into the mm test tube and leaving it for 15 h to swell and reach equilibrium swelling.

SEM analysis

The surface morphology of NIPAM-co-chitosan and NIPAM-*co*-acrylic acid gels was observed using a scanning electron microscope (HITACHI, FLEXSEM 1000, Japan).

Procedure

Material preparation

The material preparation stage was carried out by weighing 11 g of NIPAM for one synthesis and weighing 16.5 g of chitosan and 6.9 g of acrylic acid for the four synthesis variables. Then, 0.14 g of TEMED and 20 mL of APS were used for one synthesis and then followed by the preparation of MBAA cross-linker with a 30 mmol/L concentration.

NIPAM purification

NIPAM purification is carried out by preparing

benzene as a solvent (510 mL), NIPAM crystals (300 g), and *n*-hexane solution (5 L). Then, the benzene and NIPAM were mixed and stirred until the NIPAM was homogeneously dissolved. The NIPAM and benzene solution was divided into six Erlenmeyer pieces. Then, *n*-hexane was added into the Erlenmeyer so that the total solution was from NIPAM, benzene, and approximately 1 L of hexane. Each Erlenmeyer was closed tightly with plastic film and put in the refrigerator for 1 d. After being cooled, the NIPAM crystals were separated using a vacuum filter and then dried in a vacuum oven for 2 h at 50 °C. NIPAM monomer is ready to be used for copolymer production.

Gels synthesis

Synthesis of NIPAM-*co*-acrylic acid and NIPAM-*co*-chitosan gel. Solution A was synthesized by first dissolving NIPAM, acrylic acid, MBAA, and Na_2SO_3 accelerator in distilled water until a volume of 100 mL was attained. This solution was then put into a four-neck flask and heated to 30 °C to synthesize NIPAM-*co*-acrylic acid. Followed by homogenizing the solution by purging it with 500 mL/min of N_2 gas while vigorously swirling the solution for 10 min. After 10 min, combine the 2 mmol/L initiator with 20 mL of distilled water to make solution B, then purge the mixture with N_2 gas and wait for 30 min. Mix solutions A and B with a stirrer and continue purging with N_2 gas, then wait 15 s until thoroughly mixed. The polymerization reaction was varied from 10–70 °C for 6 h. After 6 h, wash the product gel with distilled water for a week. The synthesis of NIPAM-*co*-chitosan copolymers is the same as the synthesis of copolymers NIPAM-*co*-acrylic acid except using TEMED as an accelerator.

Concentrations of NIPAM:acrylic acid and NIPAM:chitosan employed in this study were 8:2 and 9:1, with a total monomer concentration of 1,000 mmol/L. The total volume of the solution is 120 mL, with a cross-linker concentration (MBAA) of 30 mmol/L, an accelerator concentration of 10 mmol/L, and an initiator concentration of 2 mmol/L. The blending composition of NIPAM-*co*-acrylic acid:NIPAM-*co*-chitosan is 1:1. Various synthesis temperature was used, i.e., 10–70 °C.

Blending of NIPAM-*co*-chitosan and NIPAM-*co*-acrylic acid gels. The first step was to dry the NIPAM-*co*-chitosan and NIPAM-*co*-acrylic acid dry gel in the oven at 40 °C for 24 h. Then crush the NIPAM-*co*-chitosan and NIPAM-*co*-acrylic acid copolymer sheets with a blender to make them powder with 180 mesh size. Finally, mix NIPAM-*co*-chitosan powder with NIPAM-*co*-acrylic acid powder in a ratio of 1:1.

Adsorption analysis

In this study, the target solution used in the adsorption process was a $PbCl_2$ solution of 10 mM. One gram of copolymer gel synthesized from various temperatures (10, 30, 50, and 70 °C) was added to a glass vial containing 20 mL of aqueous solution at a Pb^{2+} concentration of 10 mM. The glass bottles were placed in a water bath and stirred for 24 h at 10 °C to achieve equilibrium adsorption conditions. The adsorption experiment was conducted at 10 °C because at this temperature, NIPAM, utilized as a spacer agent, swells in accordance with its inherent characteristics, causing the adsorption ions to reach their maximum. To determine the concentration of cations and anions in the solution, the gel was separated from the solution by centrifuging it for 10 min after the adsorption procedure. A syringe filter was then used to filter the gel. Eq. (1) is used to determine the quantity of ions adsorbed into the gel from the concentration of cations and anions prior to and during the adsorption process.

$$Q = \frac{(C_0 - C)V}{m} \tag{1}$$

In this case, Q represents the number of cations adsorbed, C_0 represents the ion concentration in the solution before adsorption, C represents the ion concentration in the solution after adsorption, V represents the volume of the solution, and m represents the weight of the dry gel. AAS was used to determine ion concentrations.

■ RESULTS AND DISCUSSION

FTIR Analysis

Functional groups of NIPAM-co-acrylic acid

Fig. 2 and Table 1 show the FTIR analysis, which shows that NIPAM has C–H, C=O, C–O, and C=C bonds. Infrared radiation area from a wavelength of 4000 to 500 cm⁻¹ indicates the presence of bonds N–H,

C–H, C=O, and C=C, where these bonds are seen in Table 2. Meanwhile, NIPAM-*co*-acrylic acid has N–H functional groups at a wavelength of 3263.12 cm^{-1} at a concentration
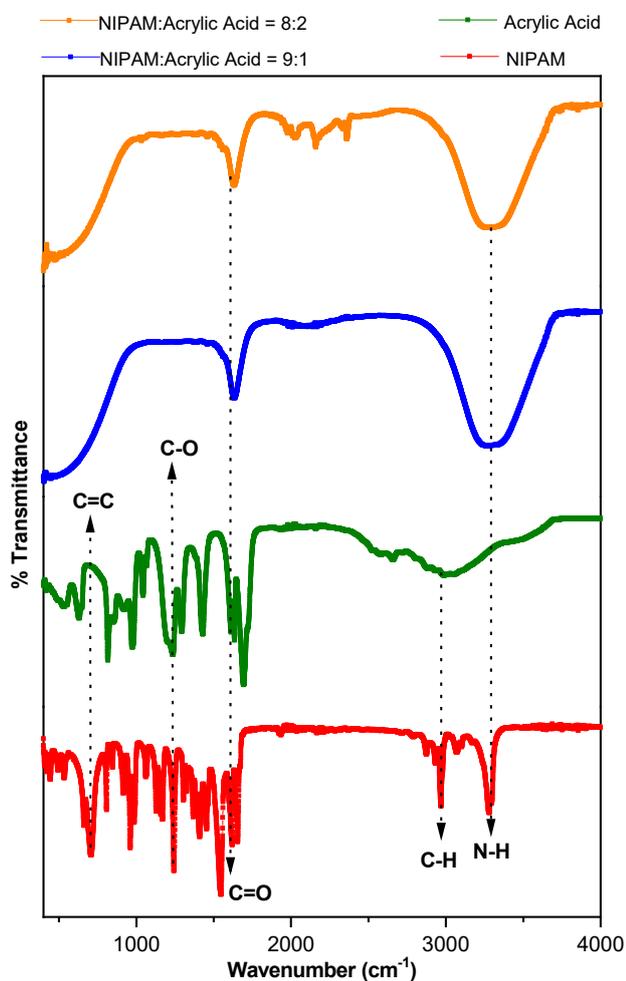
Fig 2. FTIR spectra of NIPAM, acrylic acid, and NIPAM-*co*-acrylic acid

Table 1. Wavenumber of the NIPAM functional group

No	Functional groups	Wavenumber (cm^{-1})
1	C–H	3278.86
2	C=O	1546.42
3	C–O	1243.31
4	C=C	807.33

Table 2. Wavenumber of the acrylic acid functional group

No	Functional groups	Wavenumber (cm^{-1})
1	N–H	3263.12
2	C–H	2982.22
3	C=O	1692.94
4	C=C	1234.69

of 8:2 and 3262.46 cm^{-1} at a concentration of 9:1. It has a C–O bond at a wavelength of 1635.15 cm^{-1} at a concentration of 8:2 and 1636.20 cm^{-1} at a concentration of 9:1. The synthesis of NIPAM-*co*-acrylic acid can be said to be successful if there is no vinyl group to react. This can be seen in Fig. 2 from FTIR analysis of NIPAM-*co*-acrylic acid; no sharp peaks indicate the presence of vinyl groups (C=C) as in the NIPAM spectra. These results showed the successful copolymerization reaction between NIPAM and acrylic acid.

Functional groups of NIPAM-co-chitosan

The results of the FTIR analysis of chitosan in Fig. 3 and Table 3 show that chitosan has N–H, C–H, C=O, and C=C functional groups. Fig. 3 shows the results of the FTIR analysis of NIPAM-*co*-chitosan, which has N–H, C–H, C=O, C–H, and C–O bonds. The N–H bond is located at 3271.9 cm^{-1} at a concentration of 8:2 and
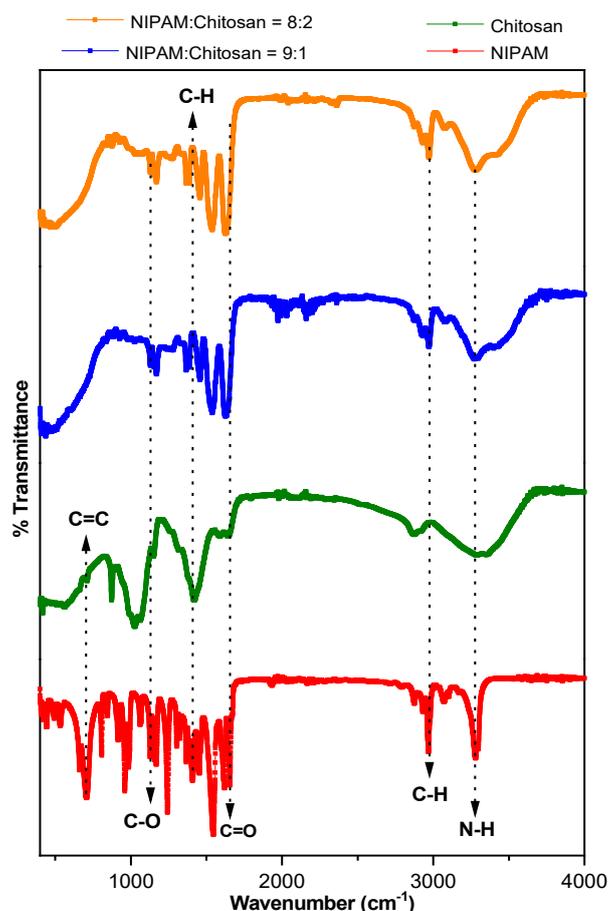
Fig 3. FTIR spectra of NIPAM, chitosan, and NIPAM-*co*-chitosan

Table 3. Wavenumber of chitosan functional groups

No	Functional groups	Wavenumber (cm^{-1})
1	N–H	3263.12
2	C–H	2982.22
3	C=O	1692.94
4	C=C	1234.69

3269.97 cm^{-1} at a concentration of 9:1. The C–H bond is located at 2989.46 cm^{-1} at a concentration of 8:2 and 2971.77 cm^{-1}. The C=O bond is located at 1634.62 cm^{-1} at a concentration of 8:2 and 1626.31 cm^{-1}. The C–H bond is located at 1386.08 cm^{-1} at concentrations of 8:2 and 1366.87 cm^{-1}. The C–O bond is located at 1173.49 cm^{-1} at concentrations of 8:2 and 1170.62 cm^{-1}. NIPAM-*co*-chitosan synthesis can be successful if there is no vinyl group to react. This can be seen in Fig. 3. In the FTIR analysis results of NIPAM-*co*-chitosan, no sharp peaks indicate the presence of vinyl groups (C=C) as in the NIPAM spectra. These results indicated that the copolymerization reaction between NIPAM and chitosan was successful.

Adsorption Analysis

Effect of synthesis temperature on ion adsorption results before and after blending

The effect of gel synthesis temperature with various monomer concentrations on the adsorption results of Pb^{2+} ions before and after blending anionic and cationic gels is shown in Fig. 4. Fig. 4 shows that the ion adsorption amount increased slightly with increasing synthesis temperature for all gel before and after blending. In addition, the adsorption value after blending on Pb^{2+} ions showed almost the same increase of around 0.15 mmol/L gel at both monomer concentrations of 8:2 and 9:1. Whereas the adsorption results after blending on Pb^{2+} ions showed an increase in adsorption values after blending of around 0.30 mmol/L which is twice compared to the adsorption before blending. This value was consistently the same at monomer concentrations of 8:2 and 9:1. When compared to previous studies, the adsorption value of heavy metal ions Pb^{2+} in blending anionic and cationic gels increased 10 times compared to the adsorption amount of divalent ions Zn^{2+} in zwitterionic DMAAPS gel [25]. The increase of the adsorption amount can be explained due to gels synthesized separately using NIPAM-*co*-chitosan and NIPAM-*co*-acrylic acid eliminate intra-chain association. NIPAM-*co*-chitosan bears ions with positive charges that interact with Cl$^-$ ions. The cation adsorption onto the gel occurs because of the availability of the active site on the surface of the NIPAM-chitosan [26-30]. The cationic charge as an active site results from the protonation of amino groups of chitosan. While NIPAM-*co*-acrylic acid contains ions with negative charges interact with Pb^{2+} ions from the solution. In addition, the ion adsorption amount of blending gels also increased than that of before blending because the
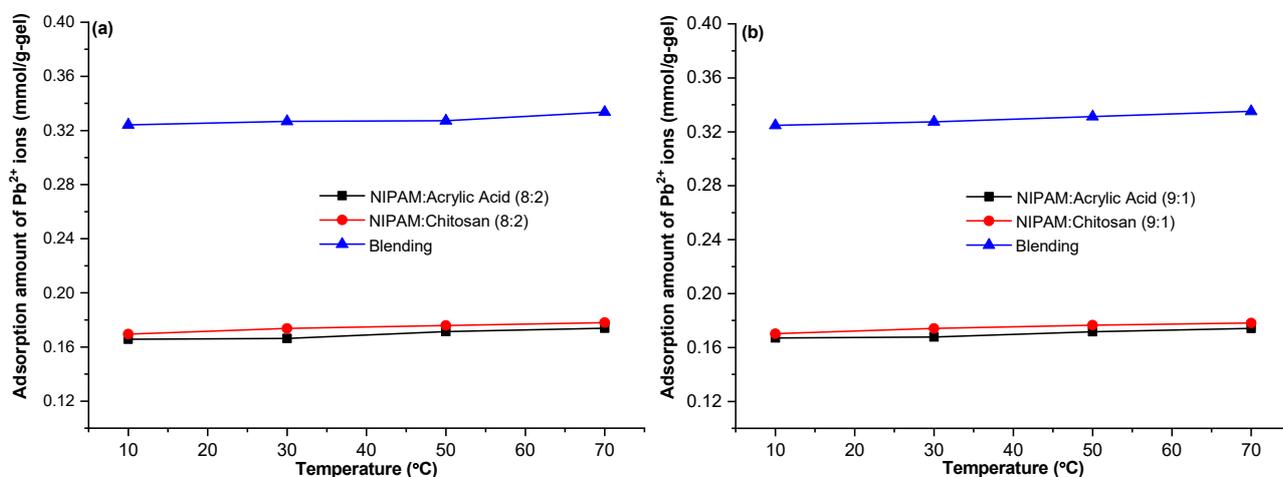
Fig 4. Adsorption of Pb^{2+} ions on NIPAM-*co*-acrylic acid and NIPAM-*co*-chitosan gel concentrations of (a) 8:2, and (b) 9:1 at various synthesis temperatures with an adsorption temperature of 10 °C

Eva Oktavia Ningrum et al.

existence of both anion and cation from gels promotes more Cl⁻ ions to interact with NIPAM-*co*-chitosan. This phenomenon may increase Pb²⁺ adsorption toward NIPAM-co-acrylic acid since Cl⁻ is the counterion for Pb²⁺ in the counterion.

Effect of monomer concentration of gels on ion adsorption

Fig. 5 shows the effect of monomer concentration on the adsorption value of each anionic and cationic gel and blending gel at various synthesis temperatures. The figure shows that the gel synthesis temperature affects the adsorption results of Pb²⁺ ions. The higher the gel synthesis temperature, the greater the adsorption value. This could be due to the formation of more porous and active sites at higher synthesis temperatures. In addition, the adsorption value of Pb²⁺ in each anionic (NIPAM-*co*-acrylic acid) and cationic (NIPAM-*co*-chitosan) gel at a concentration of 9:1 was greater than that of a monomer concentration of 8:2. This can also be seen in the blending gel shown in Fig. 5(b). This is because, at higher NIPAM concentrations, the distance between the acrylic acid in the polymer chains is farther to optimize the interaction with ions in solution even though the active ionic groups in the gel with a concentration of 8:2 are greater than those with a concentration of 9:1. From the adsorption results, it can be concluded that optimal adsorption values can be obtained by blending anionic and cationic gels, increase NIPAM concentration and synthesis temperature.

Ion selectivity on blending gels

The selectivity of mixing anionic (NIPAM-*co*-acrylic acid) and cationic (NIPAM-*co*-chitosan) gel toward different divalent ions of Fe²⁺, Ni²⁺, and Pb²⁺ is illustrated in Fig. 6. The order of the adsorption amount is Pb²⁺ > Fe²⁺ > Ni²⁺. This phenomenon followed the Hofmeister series in which states that an isoelectric covalent ion's hydration capacity, or the amount of force it exerts on water molecules, is inversely proportional to the radius of the ion and its surface charge dens. The maximum amount of Pb²⁺ adsorbed by blending anionic (NIPAM-*co*-acrylic acid) and cationic (NIPAM-*co*-chitosan) gel is 93.15 mg/g. Table 4 compares the adsorption capacity of gel with similar adsorbents that have been the subject of prior investigations.

Sedimentation Volume Analysis

Effect of synthesis temperature and gel blending on sedimentation volume

The effect of synthesis temperature on the sedimentation volume of various gels with a monomer concentration of 8:2 and adsorption temperature of 10 °C is shown in Fig. 7(a). It was found that the sedimentation volume decreased with increasing synthesis temperature. It can be seen that the sedimentation of NIPAM:chitosan was the lowest compared to NIPAM:acrylic acid and blending gel. Fig. 7(b) shows the effect of synthesis temperature on the sedimentation volume of various gels with a monomer concentration

Fig 5. Adsorption amount of Pb²⁺ in the gel (a) NIPAM-*co*-acrylic acid, NIPAM-*co*-chitosan and (b) blending them with concentrations of 8:2 and 9:1 at various synthesis temperatures with an adsorption temperature of 10 °C

Table 4. A comparison of several adsorbents toward Pb^{2+} ions

No	Adsorbent	Adsorption capacity (mg/g)	Reff.
1	Chitosan/polyethyleneimene/tailing composite	192.8	[31]
2	Polyaniline grafted chitosan	16.07	[32]
3	Structurally preorganized adsorbent	352.1	[9]
4	Humic acid-urea formaldehyde (HA-UF)	46.80	[7]
5	Immobilized dithizone on coal bottom ash	47.00	[10]
6	Nanostructure $Mg(OH)_2$	4117	[8]
7	Ligand based composite sensor material	155.3	[11]
8	Ligand based conjugate material (CMA)	196.4	[33]
9	Metal-organic framework (AMO-MOF)	472.7	[13]
10	Calix[4]arene derivatives	137.3	[14]
11	Copper (II) benzene_1,3,5-tricarboxylate (Cu-BTC) MOFs	829.6	[15]
12	Reduced graphene oxide (rGO)	217.0	[16]
13	Banana (*Musa sapientum*) peel	2.100	[17]
14	Blending NIPAM-chitosan and NIPAM-acrylic acid	93.15	This study
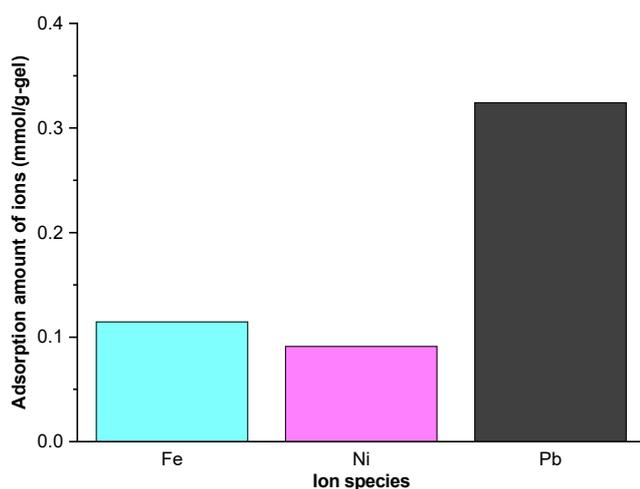
Fig 6. Adsorption amount of various ion species on blending anionic (NIPAM-*co*-acrylic acid) and cationic (NIPAM-*co*-chitosan) gels

of 9:1 and adsorption temperature of 10 °C. The sedimentation of gel with a monomer concentration of 9:1 is lower than that of a monomer concentration of 8:2. Moreover, the sedimentation volume is slightly decreased with increasing synthesis temperature.

The swelling and shrinking behavior of the gel is mainly influenced by the main constituent of the polymer chain, i.e., NIPAM and slightly influenced by the ionic monomers, i.e., chitosan which is cationic and acrylic acid which is anionic. According to Zhang et al. [34], hydrophilic properties in a gel will increase with a large number of monomers (acrylic acid) bound to NIPAM.

This also applies in Fig. 7(c). to the blending gel of NIPAM-*co*-chitosan and NIPAM-acrylic acid with a monomer concentration of 8:2 where the sedimentation volume value is higher than that of a monomer concentration of 9:1.

This is in accordance with Fig. 7(a) and 7(b) that the overall sedimentation volume value is higher at a monomer concentration of 8:2 both before blending (Fig. 7(a)) and after blending (Fig. 7(c)) as well as at a synthesis temperature of 10 °C which indicates a lower temperature synthesis, the greater the sedimentation volume value. The synthesis temperature affects the sedimentation volume because the NIPAM polymer has thermoresponsive properties at the lower critical solution temperature (LCST) at 32 °C, NIPAM will be hydrophilic at a temperature below 32 °C. Whereas NIPAM will be hydrophobic if it is above 32 °C [35-40]. The thermosensitive nature of NIPAM is what causes the sedimentation volume value at low temperatures to be higher and reach maximum swelling.

Effect of sedimentation volume on adsorption value

Fig. 8 shows the relationship between sedimentation volume and adsorption value on Pb^{2+} ions, where NIPAM-*co*-acrylic acid 8:2 has a sedimentation volume range of 7.7 to 9.7 with an adsorption value of 83–87%. For NIPAM-*co*-acrylic acid 9:1 it has a sedimentation volume range of 5.5 to 6.5 with an adsorption value of
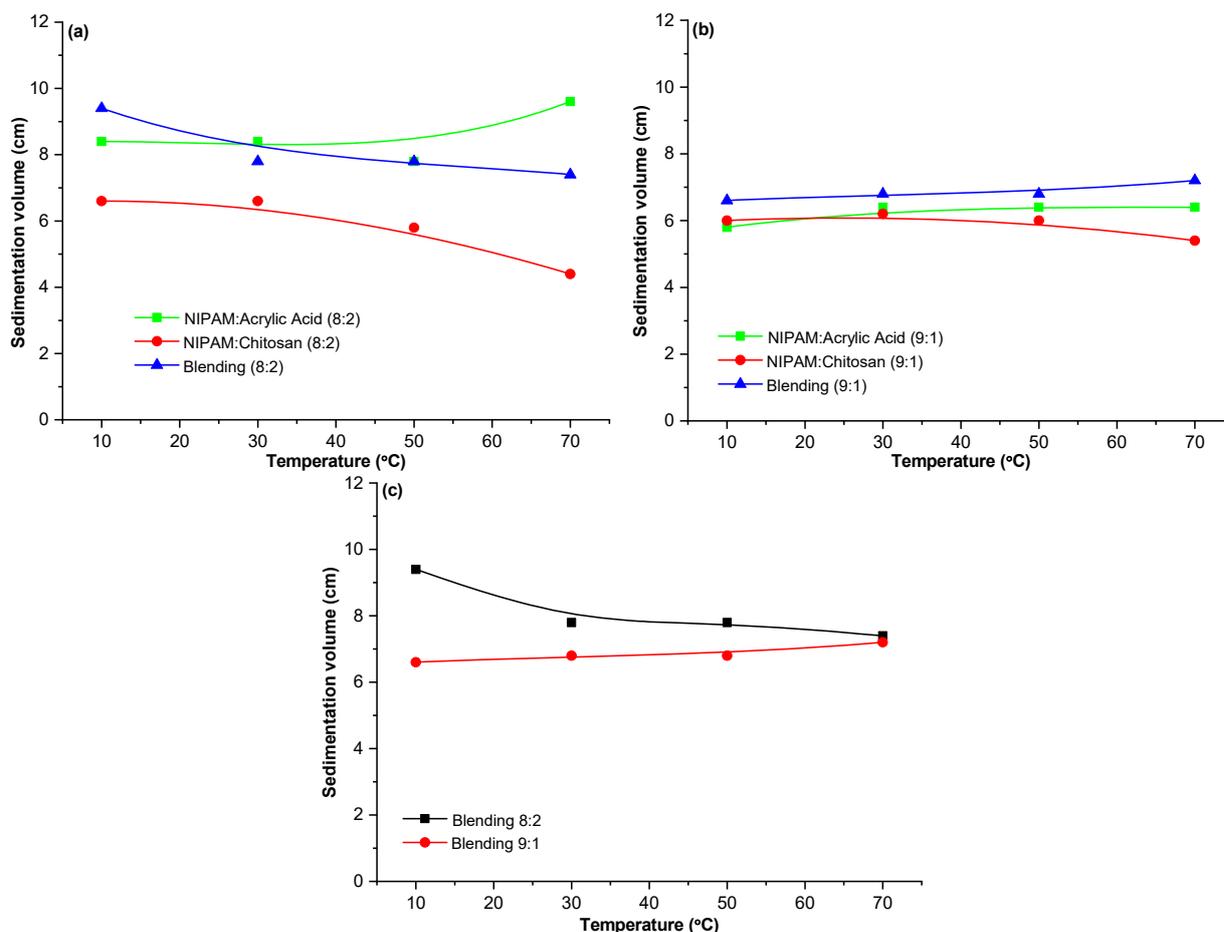
Fig 7. Effect of synthesis temperature on sedimentation volume at monomer concentration of (a) 8:2, (b) 9:1, and (c) after blending
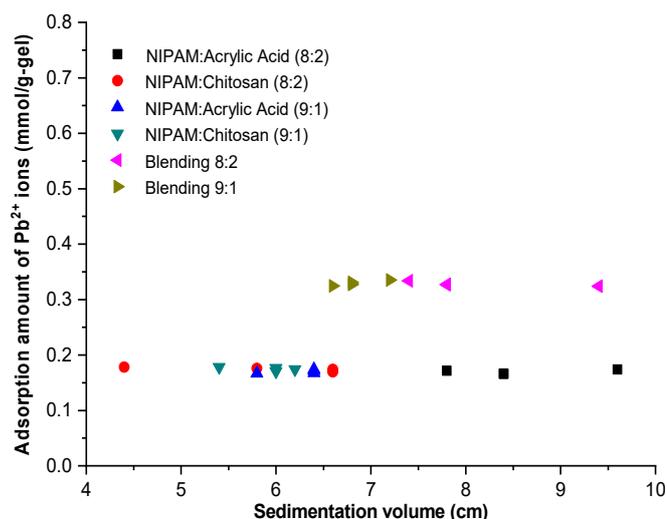
Fig 8. Correlation between sedimentation volume and adsorption value of Pb^{2+} ions at various monomer concentrations at adsorption temperature of 10 °C

82–88%. For NIPAM-*co*-chitosan 8:2 it has a sedimentation volume range between 5.7 to 6.6 with an adsorption value of 84–88%. Whereas NIPAM-*co*-chitosan 9:1 has a sediment volume range between 5.3 to 6.3 with the highest adsorption value of 85–89%. For copolymer blending 8:2 has a sediment volume range of 7.3 to 9.4 with an adsorption value of 80–84%. Meanwhile, copolymer blending 9:1 has a sediment volume range of 6.6 to 7.0. This figure showed that the adsorption ability of Pb^{2+} tends to decrease with increasing sedimentation volume.

Visual Analysis

Visual analysis of NIPAM-co-chitosan and NIPAM-co-acrylic acid gels in metal solution

Fig. 9 shows the visual results of NIPAM-*co*-chitosan gel at various synthesis temperatures and tested

at different swelling temperatures. As seen in Fig. 9, the transition phase is indicated by a color change in the solution. The polymer chain is miscible if the solution is clear (transparent). Meanwhile, if the solution is milky white in color, the component is immiscible. It can be concluded from all the visual analysis above that the resulting solution shows a transparent colored solution, which means the content of soluble waste in the NIPAM-*co*-chitosan gel. The same visual can also be seen in the NIPAM-*co*-acrylic acid gel shown in Fig. 10.

SEM Analysis

Morphology of NIPAM-co-chitosan and NIPAM-co-acrylic acid gels

The sample in Fig. 11 results from SEM analysis on NIPAM-*co*-chitosan at synthesis temperatures of 10, 30, 50, and 70 °C with a magnification of 1000×. Fig. 11(a) is NIPAM-*co*-chitosan at 10 °C, indicating no porous and only aggregates are formed. Fig. 11(b) shows NIPAM-*co*-chitosan at 30 °C, indicating some porous visible at the synthesis temperature of 50 and 70 °C.
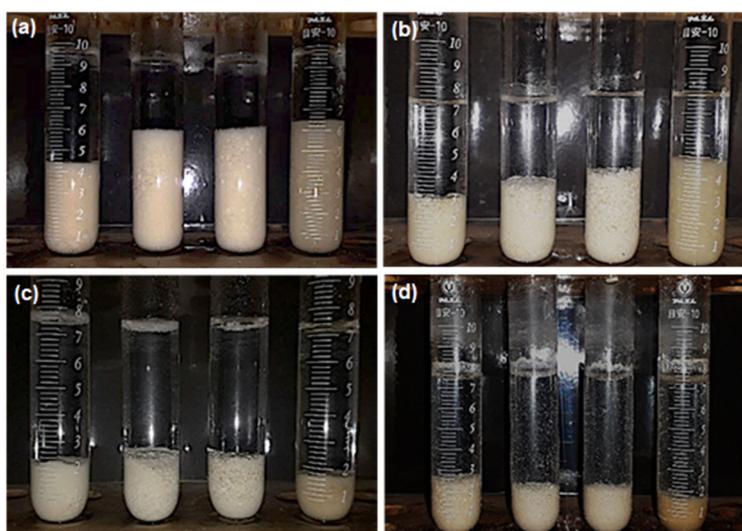
Fig 9. Visual results of NIPAM-*co*-chitosan gel at various swelling temperatures of (a) 10 °C, (b) 30 °C, (c) 50 °C, and (d) 70 °C and various synthesis temperatures of 10, 30, 50, and 60 °C (from left to right)
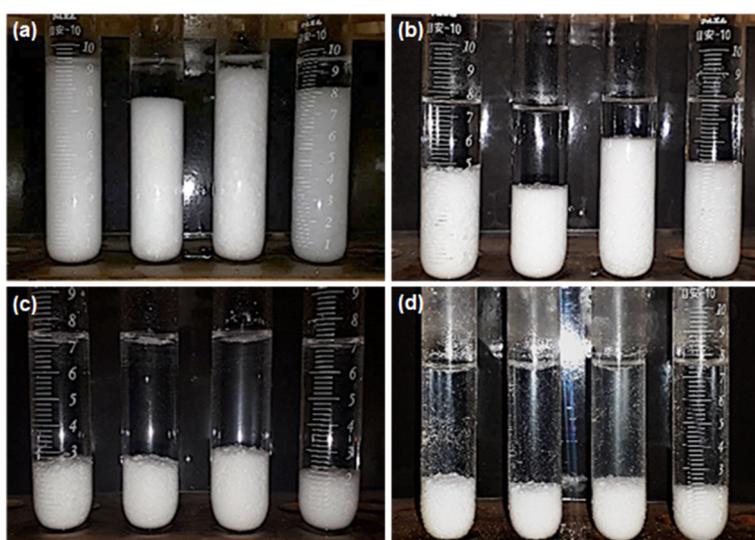
Fig 10. Visual results of NIPAM-*co*-acrylic acid gel at various swelling temperatures of (a) 10 °C, (b) 30 °C, (c) 50 °C, and (d) 70 °C and various synthesis temperatures of 10, 30, 50, and 60 °C (from left to right)
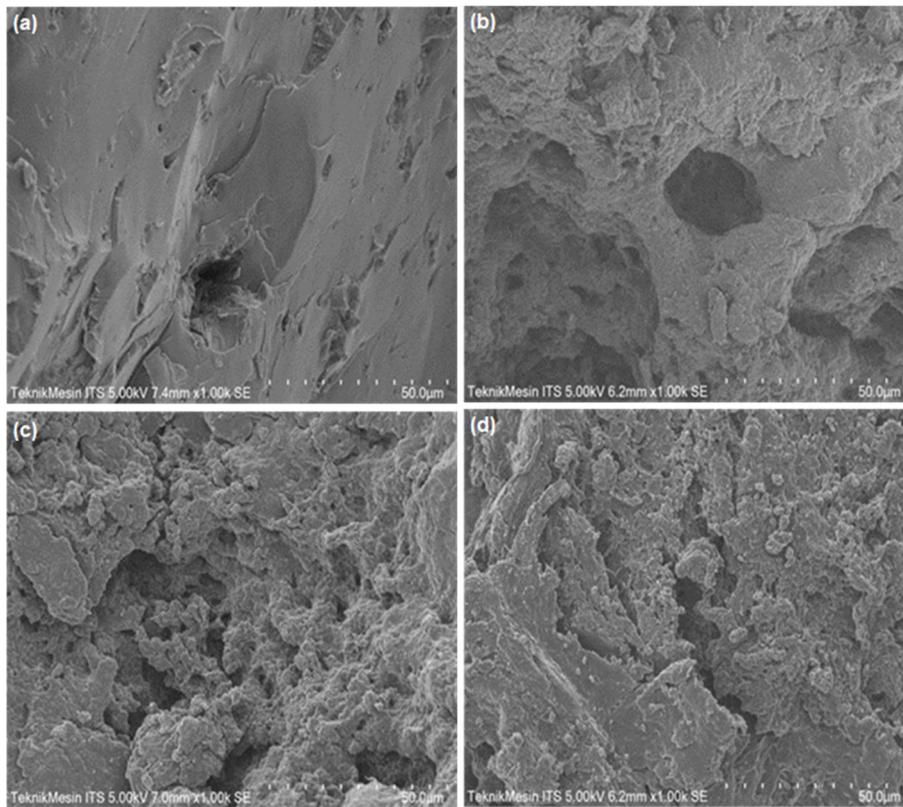
Fig 11. SEM results at NIPAM-*co*-chitosan temperature (a) 10 °C, (b) 30 °C, (c) 50 °C, and (d) 70 °C
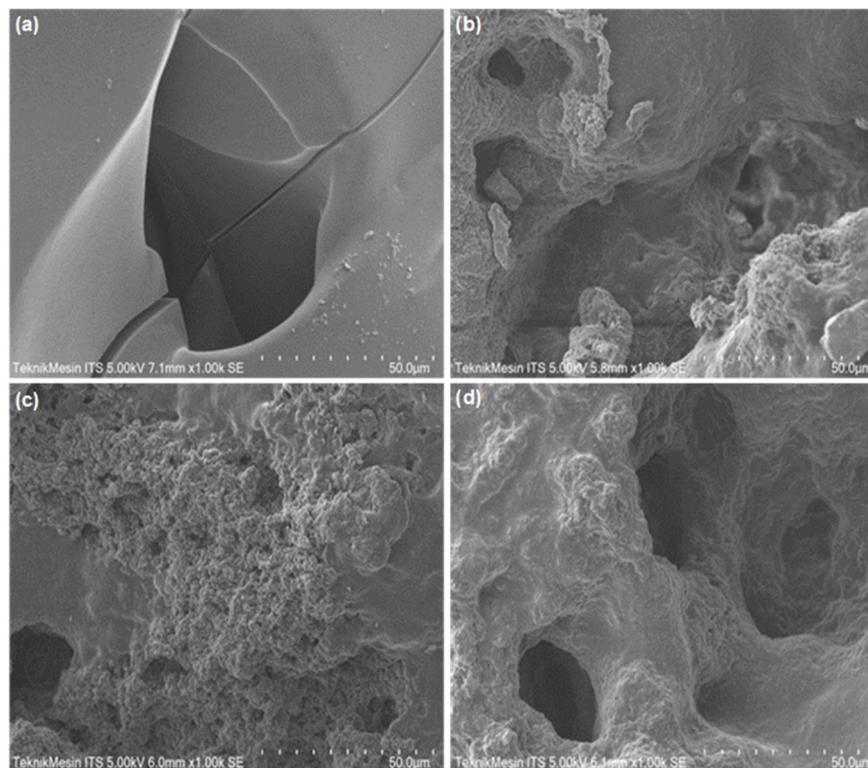
Fig 12. SEM results at NIPAM-*co*-acrylic acid temperature (a) 10 °C, (b) 30 °C, (c) 50 °C, and (d) 70 °C

However, in the NIPAM-*co*-chitosan gel, more aggregates were formed and the diameter of the porous tended to be small but scattered. The formation of porosity occurs due to the decreased solubility between NIPAM and chitosan, as it is known that NIPAM has an LCST at 32 °C. In contrast, chitosan dissolves in organic acid solutions. Thus, more porous is formed when the synthesis temperature is lower.

Additionally, larger pores are formed because of the difference in swelling properties of the NIPAM and chitosan components in the copolymer. Since chitosan does not have thermoresponsive characteristics, it expands at any temperature. NIPAM dehydrates and shrinks when the temperature reaches LCST or above, causing a phase separation between neighboring NIPAM and chitosan due to varying swelling ratios. These pores developed as a result of phase separation and shrinking of NIPAM. This is also apparent in Fig. 12, NIPAM-*co*-acrylic acid SEM test at 10, 30, 50, and 70 °C synthesis temperatures. NIPAM-*co*-acrylic acid is shown at 10 °C in Fig. 12(a), demonstrating a flat surface. NIPAM-*co*-acrylic acid is seen at 30 °C in Fig. 12(b), demonstrating numerous porous structures in addition to the synthesis temperatures of 50 and 70 °C. The higher the synthesis temperature, the bigger the porous diameter formed.

■ CONCLUSION

From the study on the effect of synthesis temperature on the performance of adsorbents based on blending anionic (NIPAM-*co*-acrylic acid) and cationic (NIPAM-*co*-chitosan) gels in the adsorption of Pb^{2+} ions, it can be concluded that from FTIR analysis of the copolymer gel NIPAM-*co*-chitosan and NIPAM-*co*-acrylic acid have several bonds including, N–H, C–H, C=O, C–O, and no peaks are indicating the presence of C=C vinyl bonds so that a synthesis NIPAM-*co*-chitosan and NIPAM-*co*-acrylic acid gel copolymers were successfully carried out. The result showed that the adsorption amount of Pb^{2+} ions blending gels increased significantly, almost twice, compared to the adsorption before blending. The adsorption amount Pb^{2+} ions increased with increasing the gel synthesis temperature. The adsorption amount follows the order of $Pb^{2+} > Fe^{2+} > Ni^{2+}$. The results of sedimentation volume analysis of NIPAM-*co*-chitosan and NIPAM-*co*-acrylic acid show that the lower the temperature, the higher the sedimentation volume. The adsorption ability of Pb^{2+} tends to decrease with increasing sedimentation volume. The higher the synthesis temperature, the larger the porous diameter formed. In addition, it can be concluded that optimal adsorption values can be obtained by blending anionic and cationic gels, increasing NIPAM concentration and synthesis temperature. In addition, from the adsorption results, it can be concluded that optimal adsorption ability can be obtained by blending anionic NIPAM-*co*-acrylic acid and cationic NIPAM-*co*-chitosan gel, increasing NIPAM concentration and synthesis temperature.

■ AUTHOR CONTRIBUTIONS

The experiment was carried out by Lulu Sekar Taji and Erlangga Ardiansyah. The calculations were carried out by Warlinda Eka Triastuti, Suprapto, Saidah Altway, and Afan Hamzah. The paper was written and corrected by Agus Surono and Eva Oktavia Ningrum. The final version of this paper was approved by all authors.

■ REFERENCES

[1] Ye, S., Zeng, G., Wu, H., Zhang, C., Dai, J., Liang, J., Yu, J., Ren, X., Yi, H., Cheng, M., and Zhang, C., 2017, Biological technologies for the remediation of co-contaminated soil, *Crit. Rev. Biotechnol.*, 37 (8), 1062–1076.

[2] Hartoyo, D., Soepardjo, A.H., Alamsyah, A.T., and Herlambang, A., 2018, "Marine Ecosystem Sustainability Post-Mine Closure Activities (Macrobenthos Dynamics Study Due to the Influence of Tailing Disposal in Buyat Bay, Minahasa, Indonesia)" in *Sustainable Future for*

Human Security: Environment and Resources, Eds. McLellan, B., Springer Singapore, Singapore, 115–126.

[3]   Tamburini, M., Badocco, D., Ercadi, R., Turicchia, E., Zampa, G., Gasparini, F., Ballarin, L., Guerra, R., Lasut, M.T., Makapedua, D.M., Mamuaja, J., Pastore, P., and Ponti, M., 2022, Bioaccumulation of mercury and other trace elements in the edible Holothurian *Holothuria* (*Halodeima*) *atra* in relation to gold mining activities in North Sulawesi, Indonesia, *Front. Mar. Sci.*, 9, 863629.

[4]   Lin, S.H., and Kiang, C.D., 2003, Chromic acid recovery from waste acid solution by an ion exchange process: Equilibrium and column ion exchange modeling, *Chem. Eng. J.*, 92 (1-3), 193–199.

[5]   Fomina, M., and Gadd, G.M., 2014, Biosorption: Current perspectives on concept, definition and application, *Bioresour. Technol.*, 160, 3–14.

[6]   Ramrakhiani, L., Ghosh, S., and Majumdar, S., 2016, Surface modification of naturally available biomass for enhancement of heavy metal removal efficiency, upscaling prospects, and management aspects of spent biosorbents: A review, *Appl. Biochem. Biotechnol.*, 180 (1), 41–78.

[7]   Sari, M.K., Basuki, R., and Rusdiarso, B., 2021, Adsorption of Pb(II) from aqueous solutions onto humic acid modified by urea-formaldehyde: Effect of pH, ionic strength, contact time, and initial concentration, *Indones. J. Chem.*, 21 (6), 1371–1388.

[8]   Amrulloh, H., Kurniawan, Y.S., Ichsan, C., Jelita, J., Simanjuntak, W., Situmeang, R.T.M., and Krisbiantoro, P., 2021, Highly efficient removal of Pb(II) and Cd(II) ions using magnesium hydroxide nanostructure prepared from seawater bittern by electrochemical method, *Colloids Surf., A*, 631, 127687.

[9]   Liang, S., Cao, S., Liu, C., Zeb, S., Cui, Y., and Sun, G., 2020, Heavy metal adsorption using structurally preorganized adsorbent, *RSC Adv.*, 10 (12), 7259–7264.

[10]   Huda, B.N., Wahyuni, E.T., and Mudasir, M., 2023, Simultaneous adsorption of Pb(II) and Cd(II) in the presence of Mg(II) ion using eco-friendly immobilized dithizone on coal bottom ash, *S. Afr. J. Chem. Eng.*, 45, 315–327.

[11]   Salman, M.S., Znad, H., Hasan, M.N., and Hasan, M.M., 2021, Optimization of innovative composite sensor for Pb(II) detection and capturing from water samples, *Microchem. J.*, 160, 105765.

[12]   Jumina, J., Priastomo, Y., Setiawan, H.R., Mutmainah, M., Kurniawan, Y.S., and Ohto, K., 2020, Simultaneous removal of lead(II), chromium(III), and copper(II) heavy metal ions through and adsorption process using C-phenylcalix[4]pyrogallolarene material, *J. Environ. Chem. Eng.*, 8 (4), 103971.

[13]   Wang, H., Wang, S., Wang, S., Fu, L., and Zhang, L., 2023, Efficient metal-organic framework adsorbents for removal of harmful heavy metal Pb(II) from solution: Activation energy and interaction mechanism, *J. Environ. Chem. Eng.*, 11 (2), 109335.

[14]   Busroni, B., Siswanta, D., Jumina, J., Santosa, S.J., and Anwar, C., 2022, Adsorption of Pb(II) on calix[4]arene derivatives: Kinetics and isotherm studies, *Indones. J. Chem.*, 22 (6), 1480–1489.

[15]   Weyrich, J.N., Mason, J.R., Bazilevskaya, E.A., and Yang, H., 2023, Understanding the mechanism for adsorption of Pb(II) ions by Cu-BTC metal-organic framework, *Molecules*, 28 (14), 5443.

[16]   Lavelim, B., Destiarti, L., Adhitiyawarman, A., and Sasri, R., 2023, Synthesis of reduced graphene oxide-bentonite composite and its application as lead(II) ion adsorbent, *Indones. J. Chem.*, 23 (1), 1–11.

[17]   Nurain, A., Sarker, P., Rahaman, M.S., Rahman, M.M., and Uddin, M.K., 2021, Utilization of banana (*Musa sapientum*) peel for removal of Pb^{2+} from aqueous solution, *J. Multidiscip. Appl. Nat. Sci.*, 1 (2), 117–128.

[18]   Ningrum, E.O., 2019, The adsorption behaviors of thermosensitive poly(DMAAPS) grafted onto EVA porous support, *IOP Conf. Ser.: Mater. Sci. Eng.*, 543 (1), 012037.

[19]   Ningrum, E.O., Sakohara, S., Gotoh, T., Suprapto, S., and Humaidah, N., 2020, Correlating properties between sulfobetaine hydrogels and polymers with

different carbon spacer lengths, *Polymer*, 186, 122013.

[20] Ningrum, E.O., Bagus, A., Sakohara, S., Suprapto, S., and Humaidah, N., 2019, Reversible adsorption-desorption of Zn(II) and Pb(II) in aqueous solution by thermosensitive-sulfobetaine gel, *Mater. Sci. Forum*, 964, 221–227.

[21] Suharto, T., Goto, T., and Nakai, S., 2021, Simultaneous adsorption of cation and anion by thermosensitive hydrogels, *MATEC Web Conf.*, 333, 11007.

[22] Ningrum, E.O., Bagus, A., Agustiani, E., and Ni'mah, H., 2020, Thermosensitive and chitosan of crab (*Portunus pelagicus*) shells gel based adsorbent for reversible adsorption-desorption of several toxic metal ions, *IOP Conf. Ser.: Earth Environ. Sci.*, 460, 012017.

[23] Suprapto, S., Gotoh, T., Humaidah, N., Febryanita, R., Firdaus, M.S., and Ningrum, E.O., 2020, The effect of synthesis condition of the ability of swelling, adsorption, and desorption of zwitterionic sulfobetaine-based gel, *Int. J. Technol.*, 11 (2), 299–309.

[24] Ningrum, E.O., Purwanto, A., Mulyadi, E.O., Dewitasari, D.I., and Sumarno, S., 2017, Adsorption and desorption of Na^+ and NO_3^- ions on thermosensitive NIPAM-*co*-DMAAPS gel in aqueous solution, *Indones. J. Chem.*, 17 (3), 446–452.

[25] Ningrum, E.O., Murakami, Y., Ohfuka, Y., Gotoh, T., and Sakohara, S., 2014, Investigation of ion adsorption properties of sulfobetaine gel and relationship with its swelling behavior, *Polymer*, 55 (20), 5189–5197.

[26] Salman, M.S., Hasan, M.N., Hasan, M.M., Kubra, K.T., Sheikh, M.C., Rehan, A.I., Waliullah, R.M., Rasee, A.I., Awual, M.E., Hossain, M.S., Alsukaibi, A.K.D., Alshammari, H.M., and Awual, M.R., 2023, Improving copper(II) ion detection and adsorption from wastewater by the ligand-functionalized composite adsorbent, *J. Mol. Struct.*, 1282, 135259.

[27] Hasan, M.M., Kubra, K.T., Hasan, M.N., Awual, M.E., Salman, M.S., Sheikh, M.C., Rehan, A.I., Rasee, A.I., Waliullah, R.M., Islam, M.S., Khandaker, S., Islam, A., Hossain, M.S., Alsukaibi, A.K.D., Alshammari, H.M., and Awual, M.R., 2023, Sustainable ligand-modified based composite material for the selective and effective cadmium(II) capturing from wastewater, *J. Mol. Liq.*, 371, 121125.

[28] Hasan, M.N., Salman, M.S., Hasan, M.M., Kubra, K.T., Sheikh, M.C., Rehan, A.I., Rasee, A.I., Awual, M.E., Waliullah, R.M., Hossain, M.S., Islam, A., Khandaker, S., Alsukaibi, A.K.D., Alshammari, H.M., and Awual, M.R., 2023, Assessing sustainable lutetium(III) ions adsorption and recovery using novel composite hybrid nanomaterials, *J. Mol. Struct.*, 1276, 134795.

[29] Awual, M.R., 2019, A facile composite material for enhanced cadmium(II) ion capturing from wastewater, *J. Environ. Chem. Eng.*, 7 (5), 103378.

[30] Islam, A., Teo, S.H., Taufiq-Yap, Y.H., Ng, C.H., Vo, D.V.N., Ibrahim, M.L., Hasan, M.M., Khan, M.A.R., Nur, A.S.M., and Awual, M.R., 2021, Step towards the sustainable toxic dyes removal and recycling from aqueous solution-A comprehensive review, *Resour., Conserv. Recycl.*, 175, 105849.

[31] Zhang, Y., Haris, M., Zhang, L., Zhang, C., Wei, T., Li, X., Niu, Y., Li, Y., Guo, J., and Li, X., 2022, Amino-modified chitosan/gold tailings composite for selective and highly efficient removal of lead and cadmium from wastewater, *Chemosphere*, 308, 136086.

[32] Karthik, R., and Meenakshi, S., 2015, Removal of Pb(II) and Cd(II) ions from aqueous solution using polyaniline grafted chitosan, *Chem. Eng. J.*, 263, 168–177.

[33] Awual, M.R., 2019, Mesoporous composite material for efficient lead(II) detection and removal from aqueous media, *J. Environ. Chem. Eng.*, 7 (3), 103124.

[34] Zhang, J., Chu, L.Y., Li, Y.K., and Lee, Y.M., 2007, Dual thermo-and pH-sensitive poly(*N*-isopropylacrylamide-co-acrylic acid) hydrogels with rapid response behaviors, *Polymer*, 48 (6), 1718–1728.

[35] Qi, M., Li, G., Yu, N., Meng, Y., and Liu, X., 2014, Synthesis of thermo-sensitive polyelectrolyte

complex nanoparticles from CS-*g*-PNIPAM and SA-*g*-PNIPAM for controlled drug release, *Macromol. Res.*, 22 (9), 1004–1011.

[36] Meng, T., Xie, R., Chen, Y.C., Cheng, C.J., Li, P.F., Ju, X.J., and Chu, L.Y., 2010, A thermo-responsive affinity membrane with nano-structured pores and grafted poly(*N*-isopropylacrylamide) surface layer for hydrophobic adsorption, *J. Membr. Sci.*, 349 (1-2), 258–267.

[37] García-Peñas, A., Biswas, C.S., Liang, W., Wang, Y., Yang, P., and Stadler, F.J., 2019, Effect of hydrophobic interactions on lower critical solution temperature for poly(*N*-isopropylacrylamide-*co*-dopamine methacrylamide) copolymers, *Polymers*, 11 (6), 991.

[38] Singh, R., Deshmukh, S.A., Kamath, G., Sankaranarayanan, S.K.R.S., and Balasubramanian, G., 2017, Controlling the aqueous solubility of PNIPAM with hydrophobic molecular units, *Comput. Mater. Sci.*, 126, 191–203.

[39] Bokias, G., Hourdet, D., Iliopoulos, I., Staikos, G., and Audebert, R., 1997, Hydrophobic interactions of poly(*N*-isopropylacrylamide) with hydrophobically modified poly(sodium acrylate) in aqueous solution, *Macromolecules*, 30 (26), 8293–8297.

[40] Ohnsorg, M.L., Ting, J.M., Jones, S.D., Jung, S., Bates, F.S., and Reineke, T.M., 2019, Tuning PNIPAm self-assembly and thermoresponse: Roles of hydrophobic end-groups and hydrophilic comonomer, *Polym. Chem.*, 10 (25), 3469–3479.